Wind Engineering Joint Usage/Research Center
FY2017 Research Result Report

Research Field: Wind disaster and wind resistant design
Research Year: FY2017
Research Number: 172003
Research Theme: Interference effects on the aero-dynamic and aero-elastic behaviors of a high-rise building due to a vibrating neighboring building

Representative Researcher: Yuan-Lung Lo

Budget [FY2017]: 270,000Yen

*There is no limitation of the number of pages of this report.
*Figures can be included to the report and they can also be colored.
*Submitted reports will be uploaded to the JURC Homepage and etc.....

1. Research Aim

This research is based on the results of JURC 2015 and 2016 projects and mainly focused on re-checking the aero-elastic behavior of the principal building if there exists an existing vibrating interfering building. The main methodology adopted for this research is vibration measurement tests in a well simulated boundary layer flow. The square cross section model and the tapered model are selected for the principal and the interfering building has identical geometric size as the square one. In order to make the interfering building model vibrating, a base with changeable rod is designed to exhibit the same structural frequency as the principal building model. In order to reduce the disturbance to the turbulence in the lower part of both buildings, the height of the base mechanism is limited within 30 mm and the width is the same as the width of the square model.

2. Research Method

The aero-elastic vibration test is conducted in the 18 × 1.8 × 2.2 m boundary layer wind tunnel of Wind Engineering Research Center at Tokyo Polytechnic University. A 1/400 scale turbulent flow over a sub-urban terrain with a power law index exponent for mean velocity profile of 0.19 is simulated with properly equipped spires, saw barriers, and roughness blocks. For the aeroelastic vibration test, two rigid base-pivoted aero-elastic models, square and tapered, are manufactured for the role of the principal building. The square prism model is 0.07 m in both width (*B*) and depth (*D*) and 0.56 m in height (*H*), which make the aspect ratio (*H/B*) 8. The tapered model is 0.04 m in width on the roof-top and 0.10 m in width on the bottom. The height is the same as the square one and the aspect ratio (height to the averaged width) is also 8. Both the two principal models are manufactured with the same volume in order to have a basic comparison level. The tapered model has been proven to efficiently reduce the projected wind force when they are considered in an isolated condition (Kim et al., 2014, 2015, 2016). The tapered model in this study is also referred to Model IV by Kim et al. (2016). Fundamental modal information of the two principal models is listed in Table 1. The fundamental frequencies in along-wind (longitudinal) and across-wind (lateral) directions are tuned to 6.0 Hz based on free vibration tests. The damping ratios are kept under or equal to 0.6% in both directions for two models and the generalized masses are about 0.11 kg. The corresponding mass-damping parameter is determined by

$$\delta = \frac{M\xi}{\rho B^2 H} \tag{1}$$

where ρ is the air density. M is the generalized mass. ξ is the damping ratio. For the rigid base-pivoted aeroelastic model in this study, the mass-damping parameters for three models are in the range of 0.2 to 0.3, which is slightly lower than the range of typical full scale high-rise buildings (0.4 – 0.6) and can be converted to Scruton numbers of 0.7 to 1.0 based on the linear mode shape assumption of its rigid elastic feature. Generally speaking, in this range of lower Scruton numbers, the across-wind response of an isolated square prism model will increase significantly when the reduced velocity rises to values larger than 9 or 10. Furthermore, from Table 1, the parameters in these two models are intentionally made the same or similar in order to reduce the possible differences in reducing dynamic response not by the shape changes. In real situations, the tapered building may be stiffer than the square buildings. The displacement signals of both directions are recorded by two laser sensors at the sampling rate of 550 Hz. The sampling length is 16,384 for one sample record and the ensemble size is 10 in order to obtain a statistical result.

Table 1 Model information for wind tunnel test

Principal model	Square (SQ)	Tapper (TA)
Height (H)	0.56	0.56
Depth (D)	0.07	0.10 (bottom) 0.04 (top)
Width (B)	0.07	0.10 (bottom) 0.04 (top)
H/B_{ave}	8	8
Helical angle	0°	0°
$f_{n,x}$ (Hz)	6.0	6.0
$f_{n,y}$ (Hz)	6.0	5.9
ξ_x (%)	0.6	0.6
ξ_y (%)	0.6	0.5
M^* (g)	106	110
δ_x	0.2	0.2
δ_y	0.2	0.2

The interfering building model is made of Basald wood and has the identical size as the square prism model. In order to make the interfering model vibrate at the same frequency of the principal model, the diameter of the rod is adjusted and free vibration test is carried out. Fig. 1 shows the rod inside the wooden surface of the model and the integrated model. The interference locations of interest are focused on those considered significant in the surrounding area (Fig. 2). Both the principal and interfering models are orientated with one face normal to the wind when both tests are carried out. Five location series including the upwind series, the oblique-upwind series, the side series, the oblique-downwind series and the downwind series are selected for observing different interference mechanisms.

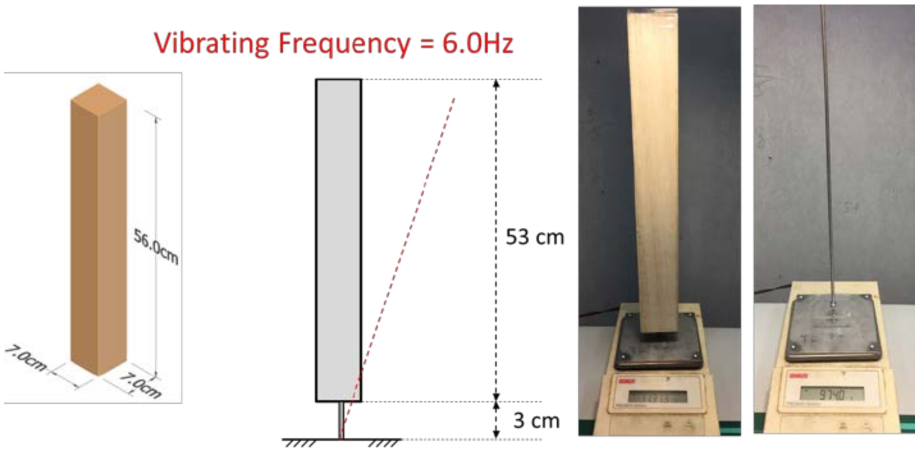

Fig. 1 Geometric size and photos of interfering model

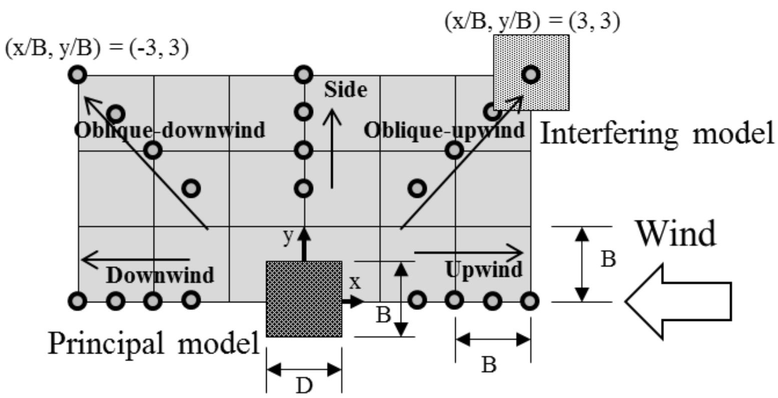

Fig. 2 Diagram of interference location series

3. Research Result

Interference effects on high-rise buildings with caused by a vibrating neighboring building have been examined in this study. For fluctuating response in the across-wind direction, according to the current estimation results from experiments, no significant difference between the cases with rigid interfering model and those cases with vibrating interfering model. The tendency in each location series is similar except for the location series of upwind locations. A slight difference can be found. For 1-sec peak acceleration values, the 1-sec averaging acceleration response was calculated from second-order differentiation of displacement; however, the distribution in terms of reduced velocities show the maximum peak acceleration occur at two frequency humps for the location series of oblique-upwind and downwind locations. Fig. 3 – Fig 6 shows both the square and the tapered models for fluctuating displacement and 1-sec peak acceleration values. However, due to page limitation, only oblique-upwind and downwind location series are plotted.

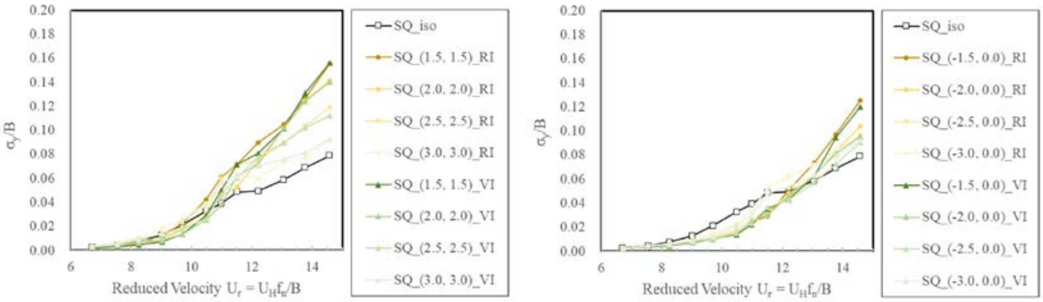

Fig. 3 SQ cases for fluctuating displacement (left: oblique-upwind; right: upwind)

(RI: rigid interfering model; VI: vibrating interfering model)

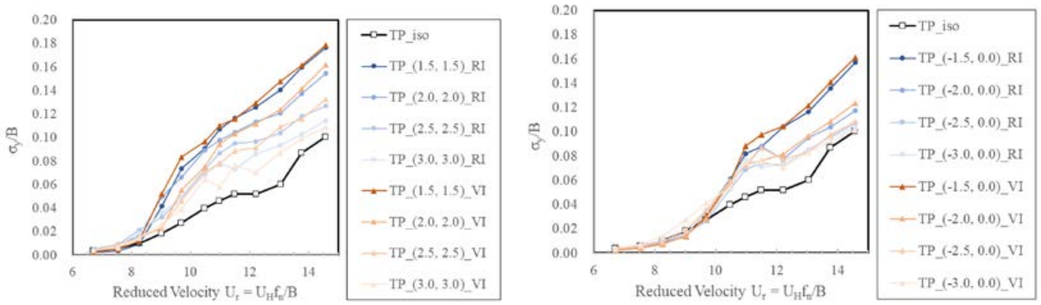

Fig. 4 TP cases for fluctuating displacement (left: oblique-upwind; right: upwind)

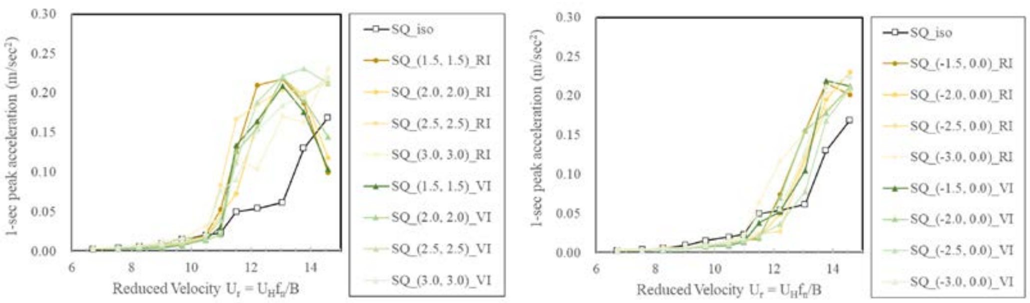

Fig. 5 SQ cases for 1-sec peak acceleration (left: oblique-upwind; right: upwind)

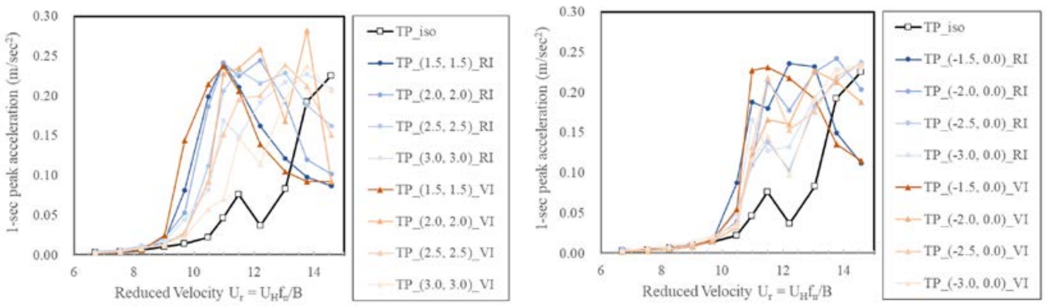

Fig. 6 TP cases for 1-sec peak acceleration (left: oblique-upwind; right: upwind)

4. Published Paper etc.

[Underline the representative researcher and collaborate researchers]

[Published papers]

1. Yuan-Lung Lo, Yong Chul Kim, Interference Effect on Wind-induced Response Characteristics of High-rise Buildings. J. Wind Eng. Ind. Aerodyn. (Under-reviewing)

2. Yuan-Lung Lo, Yong Chul Kim, Akihito Yoshida, 2017 Sep., Effects of aerodynamic

modification mechanisms on interference from neighboring buildings, Journal of Wind Engineering and Industrial Aerodynamics, Vol.168, p271-287. (SCI)
3. Yuan-Lung Lo, Yong Chul Kim, Yi-Chao Li, 2016 Dec., Downstream interference effect of high-rise buildings under turbulent boundary layer flow, Journal of Wind Engineering and Industrial Aerodynamics, Vol.159, p19-35. (SCI)

[Presentations at academic societies]
1. Yuan-Lung Lo, Yong Chul Kim, Yi-Chao Li, Akihito Yoshida, Dec. 2017, Interference Effect of High-rise Buildings, 2017 JRPES and JURC Seminar. Tamsui, Taiwan.
2. Yuan-Lung Lo, Yong Chul Kim, Akihito Yoshida, Jul 2017, Aero-elastic Behavior of High-rise Buildings under Downstream Interference Effects, European and African Conference on Wind Engineering 2017. Liege, Belgium.
3. Yuan-Lung Lo, Yong Chul Kim, Akihito Yoshida, Mar., 2017, Effects of Aerodynamic Modification Mechanisms on Interference from Neighboring Buildings, 2017 JURC Workshop. Kanagawa, Japan.
4. Yuan-Lung Lo, Yong Chul Kim, Yi-Chao Li, Oct 2016, Downstream Interference Effect of High-rise Buildings under Turbulent Boundary Layer Flow, 14th International Symposium on Structural Engineering. Beijing, China.
5. Yuan-Lung Lo, Yong Chul Kim, Jul 2016, Downstream Interference Effects between Two Identical Square Buildings under Turbulent Boundary Layer Flow, 2016 Asian Conference on Civil, Material and Environmental Sciences. Sapporo, Japan.
6. Yuan-Lung Lo, Yong Chul Kim, Yi-Chao Li, Jan 2016, Investigation on Aerodynamic Behavior of High-rise Buildings under Interference Effects, 2016 JURC Workshop. Kanagawa, Japan.
7. Yuan-Lung Lo, Yong Chul Kim, Nov 2015, Interference Effects on Across-wind Response of a Square Prism Based on Aero-elastic Tests, 2015 Symposium on Progress in Wind Engineering and Structural Dynamics. Tamsui, Taiwan.
8. Yuan-Lung Lo, Yong Chul Kim, Oct 2015, Investigation on Aerodynamic Damping of High-rise Buildings under Interference Effects, First Computational Mechanics Conference in Taiwan. Taipei, Taiwan.
9. Yuan-Lung Lo, Sep 2015, Interference Effect on a Square Prism Based on Aeroelastic Experiments, 126th JURC Open Seminar. Kanagawa, Japan.

[Published books]
No.

[Other]
No.

5. Research Group
   1. Representative Researcher
      Yuan-Lung Lo
   2. Collaborate Researchers
      1. Yong Chul Kim
      2. Akihito Yoshida
      3. Yi-Chao Li

6. Abstract (half page)

Interference effects on the aero-dynamic and aero-elastic behaviors of a high-rise building due to a vibrating neighboring building

Yuan-Lung Lo (Dept. Civil Eng., Tamkang University)

Summary

The main methodology adopted for this research is vibration measurement tests in a well simulated boundary layer flow. The square cross section model and the tapered model are selected for the principal and the interfering building has identical geometric size as the square one. The interfering building model is designed to exhibit the same structural frequency as the principal building model. For fluctuating response in the across-wind direction, no significant difference between the cases with rigid interfering model and those cases with vibrating interfering model. The tendency in each location series is similar except for the location series of upwind locations. A slight difference can be found. For 1-sec peak acceleration values, the 1-sec averaging acceleration response was calculated from second-order differentiation of displacement; however, the distribution in terms of reduced velocities show the maximum peak acceleration occur at two frequency humps for the location series of oblique-upwind and downwind locations. The following two figures show the SQ cases at upwind and oblique-upwind locations.

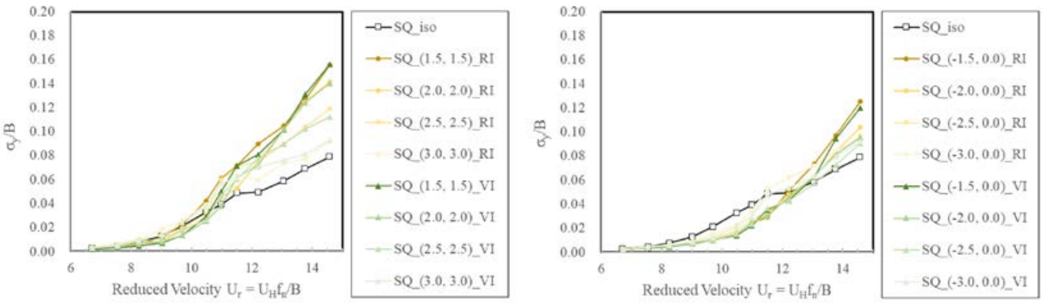

Fig. 1 SQ cases for fluctuating displacement (left: oblique-upwind; right: upwind)
(RI: rigid interfering model; VI: vibrating interfering model)

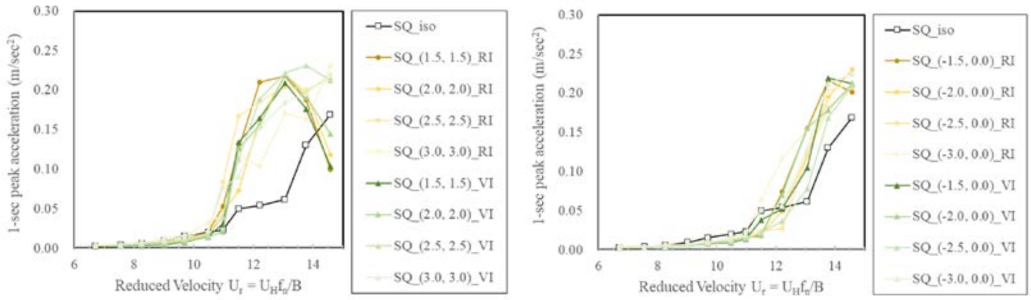

Fig. 2 SQ cases for 1-sec peak acceleration (left: oblique-upwind; right: upwind)

Interference effects on the aero-dynamic and aero-elastic behaviors of a high-rise building due to a vibrating neighboring building

Yuan-Lung Lo (Dept. Civil Eng., Tamkang University)

Summary (less than 300 words) Figures

The main methodology adopted for this research is vibration measurement tests in a well simulated boundary layer flow. The square cross section model and the tapered model are selected for the principal and the interfering building has identical geometric size as the square one. The interfering building model is designed to exhibit the same structural frequency as the principal building model. For fluctuating response in the across-wind direction, no significant difference between the cases with rigid interfering model and those cases with vibrating interfering model. The tendency in each location series is similar except for the location series of upwind locations. A slight difference can be found. For 1-sec peak acceleration values, the 1-sec averaging acceleration response was calculated from second-order differentiation of displacement; however, the distribution in terms of reduced velocities show the maximum peak acceleration occur at two frequency humps for the location series of oblique-upwind and downwind locations. The following two figures show the SQ cases at upwind and oblique-upwind locations.

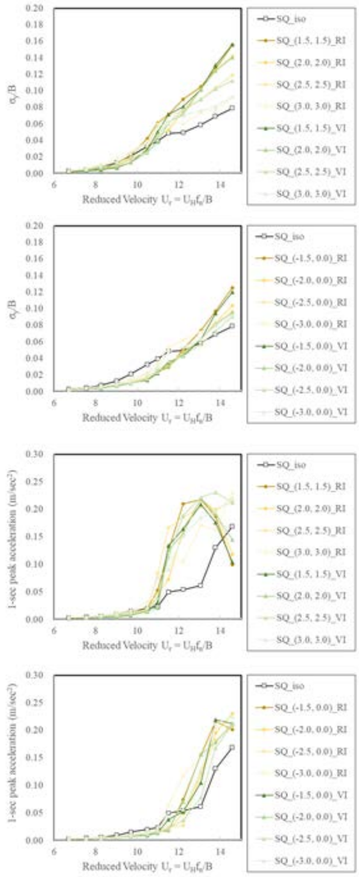

Summary

Figures